

Photometry Study of CC Andromedae



CHANDRASENA P. G. S. M.

AS/2011/2012/015

DEPARTMENT OF PHYSICAL SCIENCES
FACULTY OF APPLIED SCIENCES
RAJARATA UNIVERSITY OF SRI LANKA
MIHINTALE

Photometry Study of CC Andromedae

Chandrasena P. G. S. M

(AS/2011/2012/015)

2786

This report is submitted in partial fulfillment of the degree of

B.Sc. (4 year) degree in Applied Sciences

Faculty of Applied Sciences

Rajarata University of Sri Lanka

2017

Approved by

.....

Dr. Harshani Wijewardane

(Internal supervisor)

Senior Lecturer

Department of Physical Sciences

Faculty of Applied Sciences

Rajarata University of Sri Lanka

Mihintale

.....

Janaka Adassuriya

(External Supervisor)

Research Scientist

Astronomy & Space Science Division

Arthur C Clarke Institute

Katubedda, Moratuwa

Sri Lanka

CONTENTS

ACKNOWLEDGEMENT	ii
LIST OF ABBREVIATIONS	iii
LIST OF FIGURES	iv
LIST OF TABLES	vi
ABSTRACT	vii
CHAPTER 1	1
Introduction and overview	1
1.1 Variable stars	2
1.2 Oscillation modes in variable stars	4
1.3 CC Andromedae (CC And)	4
1.4 CCD photometry	5
1.5 UBVIR filters	6
CHAPTER 2	8
Observations	8
2.1 The 50 cm CDK Reflector and CCD Camera with Filter Wheels	8
2.2 Observation details	9
CHAPTER 3	10
Data Analysis	10
3.1 Flat-fielding	10
3.2 Centering and shifting frames	12
3.3 Aperture photometry	14
3.3.1 Detecting bright stars	14
3.3.2 Picking an aperture size	15
3.4 Light curve analysis	17
3.4.1 Lomb-Scargle Periodogram light curve analysis	17
3.4.2 Light curves of BVR bands of CC And	18
3.4.3 Fourier Analysis	19
3.4.4 Detection of oscillation periods of BVR bands of CC And	20

CHAPTER 4	22
Results.....	22
4.1 Light curves of CC And	22
4.2 Oscillation periods of CC And	25
CHAPTER 5	32
Discussion and Conclusion	32
Appendix.....	35
References.....	36

ACKNOWLEDGEMENT

There are several people I would like to thank for being helpful and in some cases essential to the completion of this thesis. First of all, I am grateful to my internal supervisor Dr. Harshani Wijewardane senior lecturer, Department of Physical Sciences, Faculty of Applied Sciences, Rajarata University of Sri Lanka, for her continuous guidance and encouragement in carrying out this work.

I would like to express my gratitude to Mr. Janaka Adassuriya, Research Scientist, Astronomy & Space Science Division, Arthur C Clarke Institute, for his inspiring guidance and constructive advices in numerous ways. Also, spending his valuable time to make this research success.

My special thanks goes to Arthur C Clarke Institute for Modern Technology (ACCIMT), Katubedda, Moratuwa for giving this valuable opportunity and I would like to thank Mount Abu observatory in India for data providing.

I sincerely thank the lecturers of the Department of Physical Sciences, Faculty of Applied Sciences, Rajarata University of Sri Lanka for their valuable support during research period.

My gratitude also goes to my loving parents for giving their kind support and encouragement during the entire period.

Finally, I would like to offer my sincere thanks to all the people who helped me to reach my target successful.

LIST OF ABBREVIATIONS

CC And – CC Andromedae

CCD – Charged Coupled Device

CDK – Corrected Dall-Kirkham

EM – Electrons Multiplying

FITS – Flexible Image Transport System

FWHM – Full Width at Half Maximum

IRAF – Image Reduction and Analysis Facility

NOAO – National Optical Astronomy Observatories

PRL – Physics Research Laboratory

PSF – Point Spread Function

SNR – Signal to Noise Ratio

LIST OF FIGURES

Figure 1.1- Classification of variable stars.....	2
Figure 1.2 - Main types of variable stars in H-R diagram.....	3
Figure 1.3- Harmonics of a string and harmonics of radial pulsations of a star.....	4
Figure 1.4- Inverted CCD photometry image of CC And.....	5
Figure 1.5- Front and back view of a CCD	6
Figure 1.6- Filter profile of UBVIR system.....	7
Figure 2.1- The dome and 50cm CDK reflector telescop.....	8
Figure 3.1- Three steps of extracting image frame.....	9
Figure 3.2- Stages of the flat field correction.....	11
Figure 3.3- CCD photometry image of a combined flat field.....	12
Figure 3.4- Reference frame	13
Figure 3.5- Frame 1 (amount of shift with respect to reference frame).....	13
Figure 3.6- Amount of shift of 538 frames of CC And star with respect to the reference frame of (B band)	13
Figure 3.7- A typical radial profile of CC And star	15
Figure 3.8- The arrangement of aperture parameters.....	16
Figure 3.9- Light curves of CC And variable star and comparison star in same plot (for B band)	18
Figure 3.10- Light curve of CC And of B band.....	18
Figure 3.11- Light curve of comparison star of B band.....	18
Figure 3.12- Light curves of CC And for B, V, R bands.....	19
Figure 3.13- Fourier fitting of B band light curve of CC And for 12 th November 2016.	20
Figure 3.14- Frequency components in B band of CC And for the 12 th November data set...21	
Figure 4.1- Light curves in B band of CC And observed on 12 th November 2016.....	22

Figure 4.2- Light curve of V band observed on 12 th November 2016.....	23
Figure 4.3- Light curve of R band observed on 12 th November 2016.....	23
Figure 4.4- Light curves in B, V and R bands of CC And observed on 12 th November 2016 in same plot.....	23
Figure 4.5 - Light curves in B band of CC And observed on 13 th November 2016.....	24
Figure 4.6- Light curves in V band of CC And observed on 13 th November 2016.....	24
Figure 4.7- Light curves in R band of CC And observed on 13 th November 2016.....	24
Figure 4.8- Light curves in B, V and R bands of CC And observed on 13 th November 2016 in same plot	25
Figure 4.9 - light curve, Fourier fitting and corresponding frequency components in B band of CC And observed on 12 th November 2016	26
Figure 4.10- light curve, Fourier fitting and corresponding frequency components in V band of CC And observed on 12 th November 2016.....	27
Figure 4.11- light curve, Fourier fitting and corresponding frequency components in R band of CC And observed on 12 th November 2016.....	28
Figure 4.12- L-S power spectra in V for the 12 th November observations of CC And with frequencies f_0, f_1, f_2 and f_3	29
Figure 4.13- L-S power spectra in B for the 12 th November observations of CC And with frequencies f_0, f_1, f_2 and f_3	30
Figure 4.14-L-S power spectra in R for the 12 th November observations of CC And with frequencies f_0, f_1, f_2 and f_3	30
Figure 5.1- Light curve in band of CC And observed on 13 th November 2016	33
Figure 5.2- Sudden variation in Comparison star and CC And star	33
Figure 5.3- Light curves of Comparison star and CC And with deviated data.....	34

LIST OF TABLES

Table 2.1 Johnson and Bessell UBVIR band pass filters and their ranges	9
Table 2.2- The observation details of CC And	9
Table 3.1- Important parameters for extraction of instrumental magnitudes	16
Table 4.1 Periodic time of CC And	29
Table 4.2 The oscillation periods of CC And for BVR filters.	31
Table 5.1 Summary of main oscillation period of CC And for 12 th November data.....	32

ABSTRACT

The Delta Scuti stars are short period variable stars which show period of less than one day. *CC Andromedae* (*CC And*) is an intrinsic variable star of Delta Scuti type, RA= 00^h 43^m 48.01^s, DEC= +42° 16' 56'', spectral type F3IV-V. This thesis describes an attempt to investigate the oscillation frequencies presented through the detail analysis of light curves of *CC And*. The main oscillation period of *CC And* is previously determined to be 0.1249078 days.

The received data of *CC And* was observed by 50 cm Corrected Dall-Kirkham reflector telescope at Mount Abu observatory in India in two consecutive nights, 12th and 13th November 2016. The photometry study of *CC And* was performed in B, V and R bands using very high sensitivity Charged Coupled Device (CCD) camera which has sensitivity to detect deci-magnitude scale changes.

The CCD photometric data, provided by Arthur C Clarke Institute for Modern Technologies, was subjected to initial corrections of bias and flat fielding using Image Reduction and Analysis Facility (IRAF) software package in UNIX operating system. The magnitudes of *CC And* in B, V and R pass bands were extracted using IRAF and high temporal resolution light curves were produced for the periodic analysis. The light curves were subjected to Fourier analysis and Lomb-Scargle periodic analysis to determine the possible oscillation periods. The determined main oscillation periods are 0.11864014 days for B, 0.12375105 days for V and 0.12956104 days for R. In addition to the main oscillation period, Fourier analysis revealed another harmonic period and Lomb-Scargle periodic analysis discovered the presence of four other oscillation frequencies of *CC And*. To the best of our knowledge this is the first time a study on the oscillation periods of B and R bands of *CC And* has been carried out and this study also shows the advantage of Lomb-Scargle periodic analysis rather than the Fourier analysis for the investigation of oscillation frequencies.

CHAPTER 1

Introduction and overview

Light that receive from the stars is the main information that can be used to study the universe. The structure and evolution of those stars can be determine through physical processes. Stars are noisy places as they have sound waves inside them. However, travelling of sound waves are not possible due to the vacuumed environment of the space. Therefore, in most cases there is no way to understand the physics behind the unobservable stellar interiors because the light of the stars radiated away from their surfaces carry no memory of its origin. Yet, there are some stars such as variable stars that the sound waves of them make the stars periodically shrink and swell, get hotter and cooler. The natural oscillation of such type of stars can be detected by performing photometry study and hence the interior of it.

This thesis presents the results of our effort aimed at the investigation of the oscillation frequency of CC Andromedae (CC And) variable star by a detail analysis of light curves of the source. This photometry study has been carried out in the formal frame of Image Reduction and Analysis Facility (IRAF) by extracting B, V and R bands. It turned out that in addition to main oscillation period, the presence of other oscillation frequencies are available for B, V and R bands of CC And. The work presented here is two fold characters;

- i. B, V and R bands were extracted from Charged Coupled Device (CCD) photometric data subjecting to initial corrections of bias and flat fielding using IRAF.
- ii. The light curves were subjected to Fourier analysis and Lomb-Scargle periodic analysis to determine the possible oscillation periods.

Hence in the continuation of this chapter, we will discuss what is it meant by a variable star, where the CC And lies. The oscillation modes in variable stars and a brief discussion on CCD photometry and UBVRI filters.

In Chapter 2 of this work, we shall give the discussion of how the data were observed for the current study. Chapter 3 is dedicated for the data analysis. How the flat fielding is done, centering and shifting frames for photometry, aperture photometry, and lastly Fourier analysis and the Lomb-Scargle periodic analysis for the observed data were discussed in this chapter. The results of B, V and R band of CC And were presented in the Chapter 4. The summery and

conclusion of what we have observed, analyzed and concluded were discussed in the Chapter 5. The script files written in IRAF were given in the Appendix.

1.1 Variable stars

Variable stars change their brightness over time, regularly or irregularly as seen from the earth [1] and they show time dependent light output. Their variation can be occurred due to rhythmic expansions and shrinks of its radius or due to some external effects like rotation or eclipse. Variable stars can be divided into two types, intrinsic variables and extrinsic variables.



Figure 1.1 - Classification of variable stars

Intrinsic variables are the ones whose luminosity physically changes due to pulsations, eruptions or through swelling and shrinking. In the extrinsic variables, the brightness change, because of being eclipsed by stellar rotation or by another star or planet. Also, variable stars can further sub divide into four main classes: the intrinsic pulsating, eruptive variables (cataclysmic stars), and the extrinsic eclipsing binary and rotating stars. Also, the pulsating and

eruptive intrinsic stars further can be divided in to many classes. These classification of variable stars [2] are given in the Figure (1.1).

The Variable stars played a major role within past decade in the story of stellar evaluation. Research on such variable stars provides many information about stellar properties, such as mass, radius, luminosity, temperature, internal and external structure, composition, and evolution. Generally, Variable stars can be analyzed using the methods of photometry, spectrophotometry and spectroscopy.

Graphical representation or plotting data are significant tool in the study of variable stars. In 1914, Ejnar Hertzsprung and Henry Norris Russell created a diagram to represent the relationship between the star's luminosity and the temperature or the color of stars (or spectral type) and the absolute magnitude. This Hertzsprung-Russell diagram (HR diagram) does not imply locations of the stars, but the star's brightness against the temperature (or color). The certain types of variable stars that can be found in the H-R diagram [3] are shown in the following Figure (1.2).

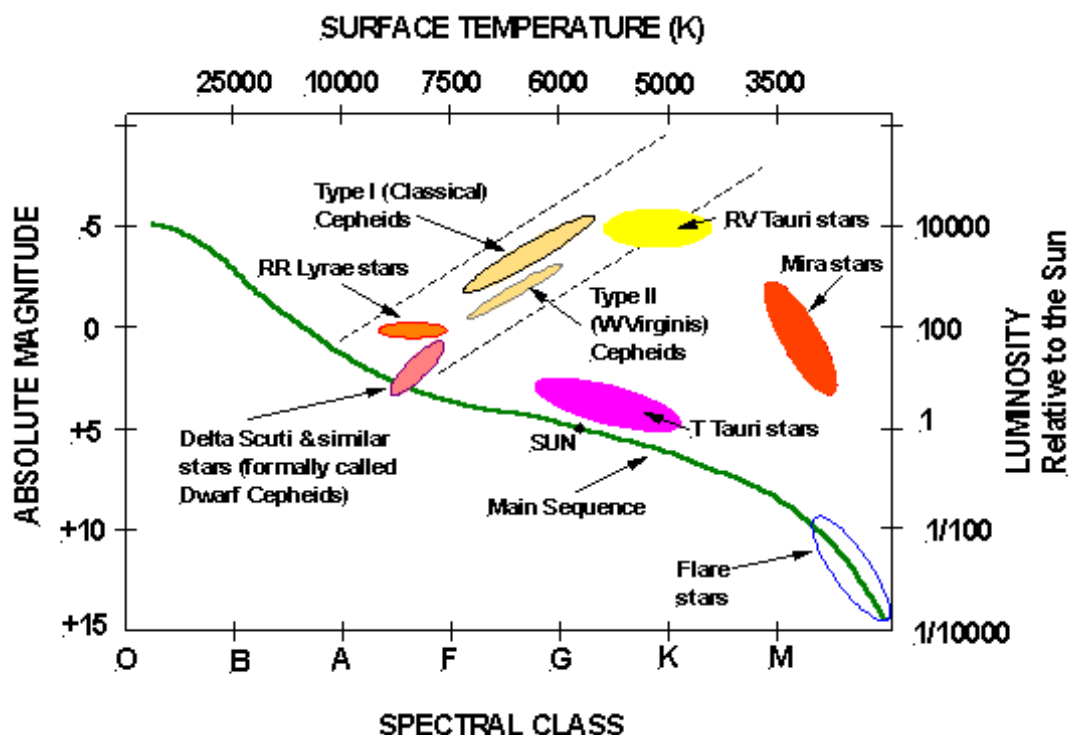


Figure 1.2 - Main types of variable stars in H-R diagram

1.2 Oscillation modes in variable stars

The oscillation modes in a variable star are similar to the oscillation modes in a vibrational string. They oscillate with fundamental mode as well as set of harmonic modes. The frequencies of the oscillation modes are caused by the sound speed of the seismic waves during their travel across the interior of the stars. The sound speed, temperature and pressure in various depth of a star can be measured with a collection of harmonics. The fundamental frequency occurs due to the expansion and contraction of the star in radial direction making the center of the star node and the surface as an anti-node. For the 1st harmonic, there is a concentric shell within the star which does not move. As it is stable, at the concentric shell it creates a node. The motions above and below the concentric shell is in anti-phase. Radial pulsations of variable star is illustrated in following Figure (1.3).

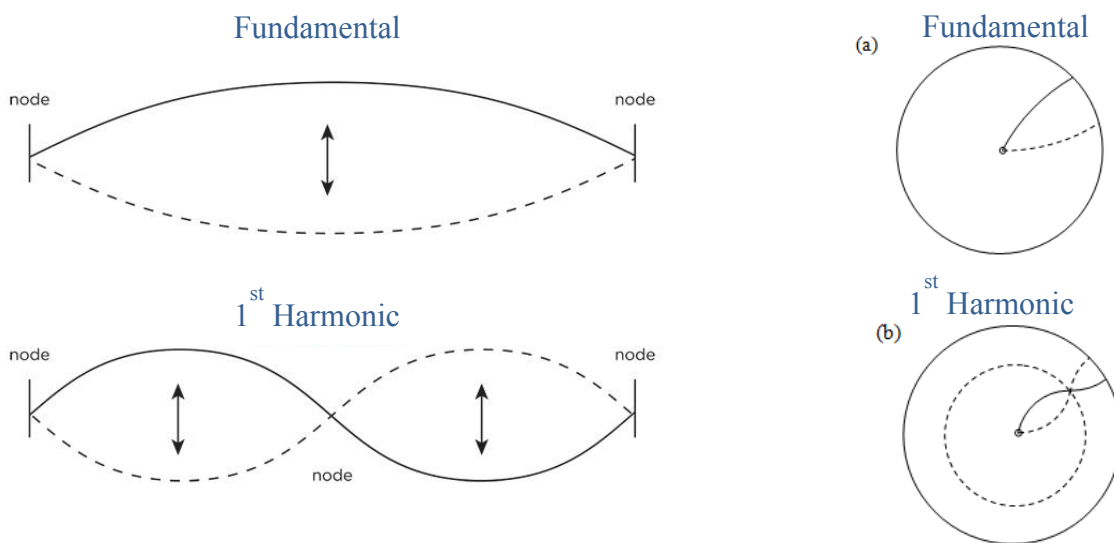


Figure 1.3 - Harmonics of a string and harmonics of radial pulsations of a star

1.3 CC Andromedae (CC And)

CC And is an intrinsic variable star of Delta Scuti type. Delta Scuti variables are short-period variables located in the main-sequence with usual definition between A2 V and FO V. Oscillation periods are between 34 minutes and 5 hours. Generally the amplitudes in light and

radial velocity are small [4]. RA= 00^h 43^m 48.01^s, DEC= +42° 16' 56'' for CC And, spectral type is F3IV-V. Its variability was firstly discovered by Eggen and Linband in 1953 [5]. The main oscillation period of 0.1249078 day was found by Wilson and Walker during 1956. Further investigation of oscillations were done by Fitch [6] who made observations of CC And with V filter and he found four pulsating periods : $P_0=0.1249078$, $P_R=0.1279623$, $P_0/2=0.06243539$ and $P_2=0.063083$ day, where the periods P_R and $P_0/2$ are resonance- excited by interaction between the fundamental P_0 and second overtone P_2 . The following Figure (1.4) shows an inverted CCD photometry image of CC And.

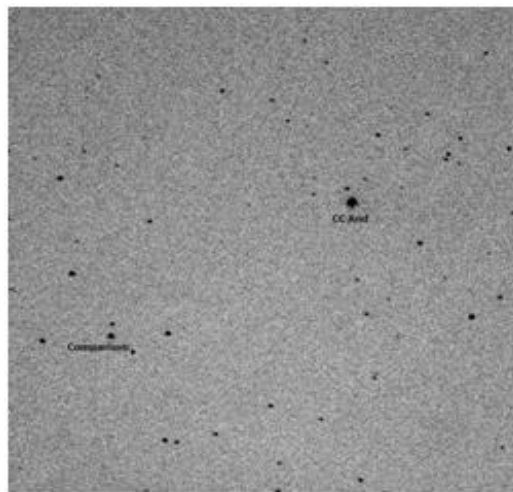


Figure 1.4 - Inverted CCD photometry image of CC And

1.4 CCD photometry

Astronomically, photometry is the science of measuring the brightness that we receive from celestial objects. In order to do this task we can use Charged Coupled Device (CCD). The CCD was invented by W.S. Boyle and G.E. Smith in 1969 which was not directly applicable in astronomical detectors. CCDs were first used in astronomy in 1976 by J. Janesick and B. Smith. Images of Jupiter, Saturn and Uranus were obtained using a CCD detector attached to the 61-inch telescope on Mt. Bigelow in Arizona [7].

CCDs are light sensitive silicon chips which are divided into a large number of electrically charged, isolated squares called “pixels”. Present day CCDs have about 512 x 512 up to 4096 x 4096 individual pixels. When light is affected on that chip, photons strike each pixel and release electrons via the photoelectric effect [8]. CCD measures how much light falls on each pixel and gives digital image as an output and each star appears as a smeared out circle covering

several pixels in that image. More brightness on Image, More photons land on it and more electrons stored in those pixels which represents a bright objects such as stars. The Figure (1.5) shows the front and back view of a CCD.

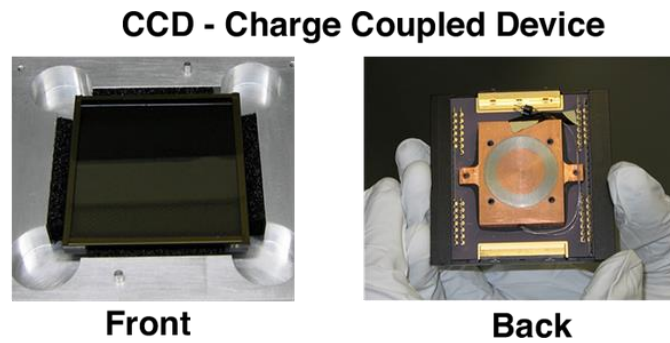


Figure 1.5 - Front and back view of a CCD

1.5 UBVR filters

Astronomical filters are a special kind of colored glass which is often placed in the path of the light. This is significant to study the specific colors of celestial objects, because it only allows light of certain wavelengths to pass through and blocks other wavelengths. There are two types of filters narrow band filters and white band filters. As the name implies narrow band filters allows small range of light and is often used to study light emitted by specific elements such as oxygen or hydrogen. Wide band filters allow a large range of wavelengths of light and it is in the area of the spectrum near visible light. U, B, V, R and I are the most commonly used set of wideband filters which was described in the 1950s by Harold Johnson and modified a few decades later by A.W.J. Cousins [9]. Also In 1990, Michael Bessell published a set of combinations of cheap optical glass filters. This kind of filters can detect faint objects with short exposure times and small telescopes, because they transmit lot of light. The Figure (1.6) shows the filter profile of UBVR system [10].

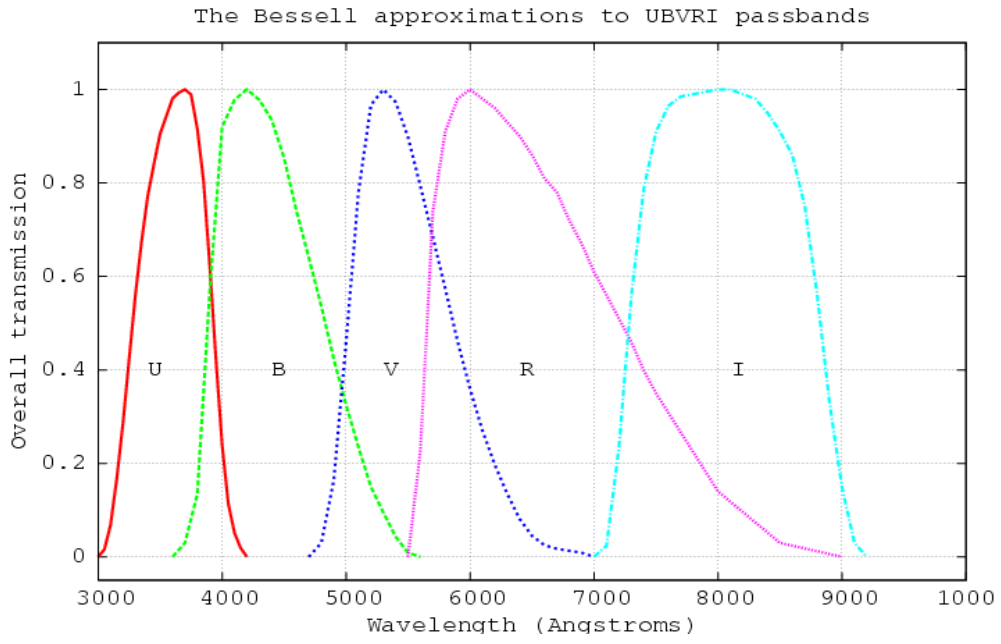


Figure 1.6 - Filter profile of UBVIR system

CHAPTER 2

Observations

The data which were used in this thesis were received from Mount Abu Infrared observatory. The observatory has carried out the data collection during 12th November and 13th November 2016. The observatory is located near the town of Mount Abu in the state of Rajasthan, India. The observatory is at 24.59 N, 72.71E and an attitude of 1680 meters with typical astronomical seeing of ~ 1.2 arc seconds and is adjacent to Guru Shikhar, the highest peak of the Aravali Range [11]. The following is a brief description about the reflector which is used at the observatory.

2.1 The 50 cm CDK Reflector and CCD Camera with Filter Wheels

The Corrected Dall-Kirkham (CDK) has a 50 cm Prolate Ellipsoid, $f/3$ primary mirror and 19 cm spherical secondary mirror with the effective focal ratio of $f/6.8$ equatorial mount telescope. The detector is 1024 x 1024 electrons multiplying (EM) CCD with a maximum cooling of -80°C and negligible read noise. The higher frame rate per second and negligible read out noise (< 1 electron with EM gain) are ideal for the observations of short period variable stars with very high time resolution. The large CCD array provides a field of view 13×13 arc minutes. In addition to the standard UBVRI filters, a set of Polaroid sheets oriented at 0, 45 and 90 degrees are also included in the system. The telescope and the dome are fully automated through the network and can be operated remotely from PRL (Physics Research Laboratory) with all functionalities including weather monitoring. Figure (2.1) shows a picture of the reflector telescope. Table (2.1) shows the standard UBVRI filters with their range.



Figure 2.1 - The dome and 50cm CDK reflector telescope

Table 2.1 Johnson and Bessell UBVIR band pass filters and their ranges

Filter	Region in EM spectrum	Wavelength Range(nm)
U	Ultraviolet	320-400
B	Blue	400-500
V	Visible	500-700
R	Red	550-800
I	Infrared	700-900

2.2 Observation details

The observations were carried out in all three bands of B, V and R and summarized observations are shown in the Table (2.2).

Table 2.2 The observation details about the photometry data of 12th and 13th November 2016 for B, V and R bands. The exposure (Exp.) time is in seconds and the coverage (Cov.) is in hours.

Date of observation	B		V		R	
	Exp. (s)	Cov. (h)	Exp. (h)	Cov. (h)	Exp. (s)	Cov. (h)
12 th Nov. 2016	4	4.12	2	4.13	2	4.11
13 th Nov. 2016	4	2.24	2	2.24	2	2.24

CHAPTER 3

Data Analysis

The photometric data were mainly analyzed by using Image Reduction and Analysis Facility (IRAF) which is a general purpose software written and supported by IRAF programming group at the National Optical Astronomy Observatories (NOAO) in Tucson, Arizona. Text and graphics were handled by Xgterm, which is a special type of terminal in IRAF. Ds9 was adopted as the display server under the UNIX system to display the CCD photometry data. All images were in FITS (Flexible Image Transport System) format. In order to find the oscillation periods, photometric data were subjected to Fourier analysis using MATLAB and Lomb-Scargle periodogram analyzing. The magnitudes for the set of image frames were extracted via three steps as shown in the Figure (3.1) to plot the light curve of CC And. These steps were discussed below.

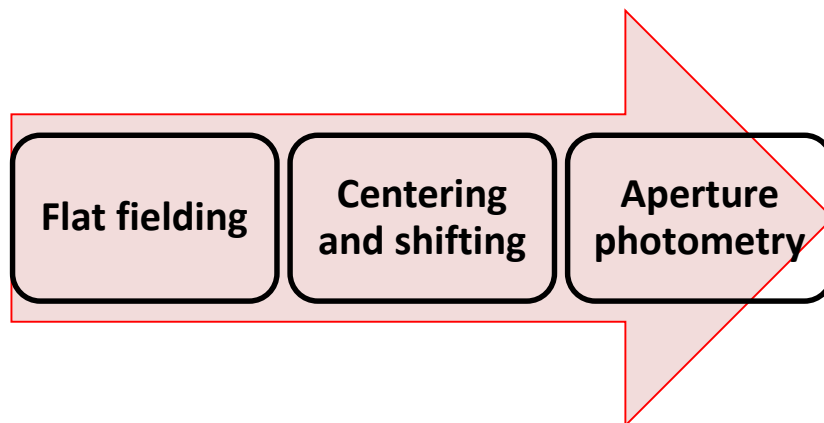


Figure 3.1 - Three steps of extracting image frames

3.1 Flat-fielding

The sensitivity of the pixels vary slightly by few percent across a CCD chip due to the limitation of the current technology and manufacturing process. Some pixels are more sensitive than the others. Also this pixel to pixel variation can change with the wavelength of incident light. This effect can be eliminated by flat field corrections [12]. Flat field frame is a picture of some homogeneous light source that covers the entire light sensitive area of the CCD. The uniform light was taken during twilights close after sunset or before sunrise. Also the sky has to be brighter than the stars and faint enough to saturate the detector.

There is a small concept behind the flat field correction. If 100 photons fall on a pixel and it generates 90 electrons, it means that the pixel is operating at an efficiency of 90%. A uniform light source should have same count of efficiencies such as [100,100,100]. But the flat field frames and final CCD images do not represent true light and each pixels operates with its own slightly different efficiencies. Consider a flat field frame affected by an uniform light source which have unequal efficiencies such as [80,90,100]. First this values should be divided by mode in order to get values close to one. Assume the mode is 100 for that frame. Then the normalized frame contain values close to one such as [0.8,0.9,1] . Finally all CCD images that have unequal efficiencies can be corrected by dividing all the CCD frames by normalized flat frame. The following Figure (3.2) shows the main stages behind the flat field correction.

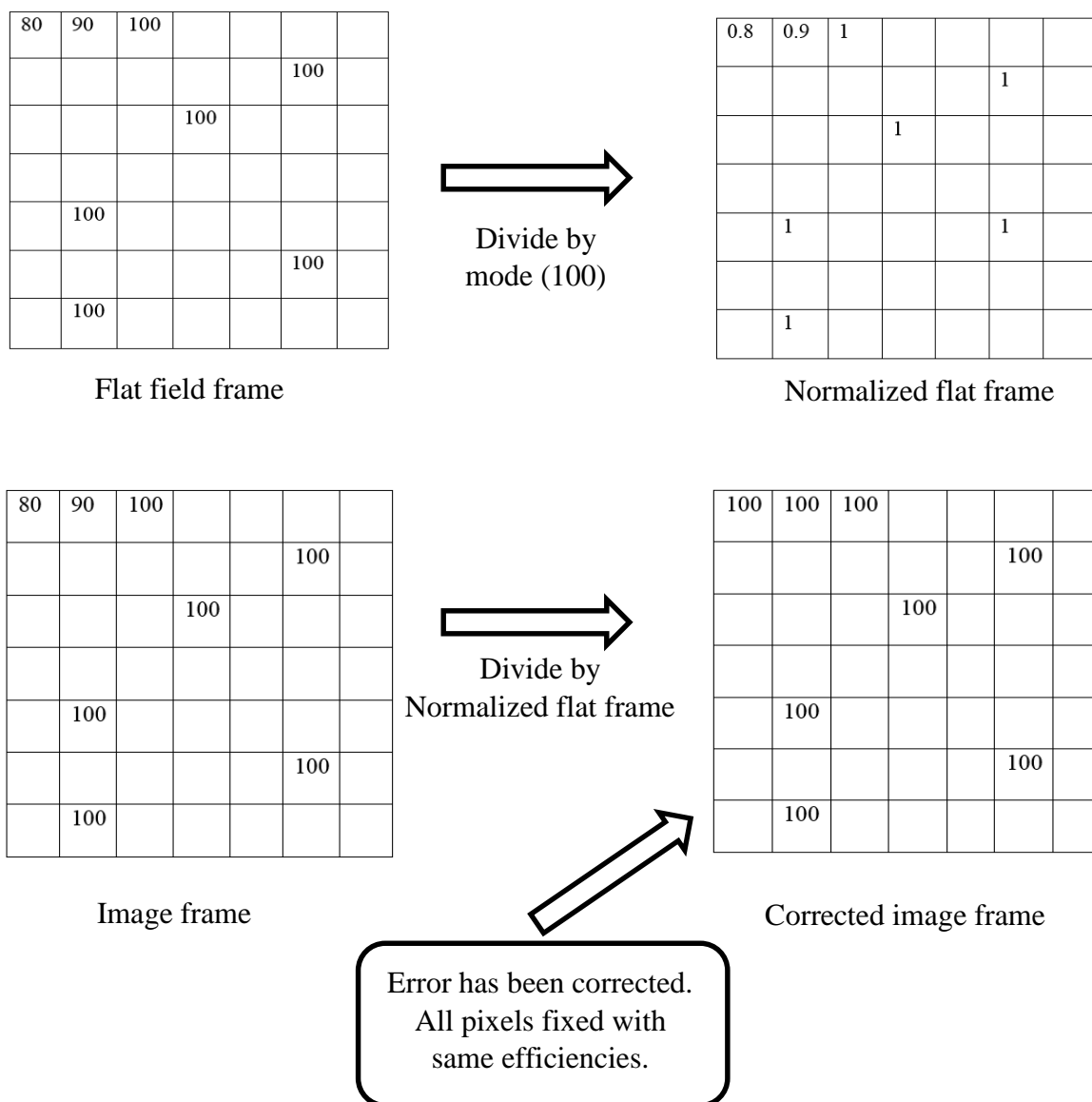


Figure 3.2 - Stages of the flat field correction

Several frames were taken to create a good flat field and those frames were combined into one flat-field for each filters separately using the task `*imcombine` in IRAF workplace. Normalization value (mode) was determined for the flats by the task `*imstat` and then it was subjected to the task `*imarith` to obtain the normalized flat field frame. Again each image frame was divided by normalized flat using `*imarith` to correct uneven illumination of the CCD. The Figure (3.3) gives an image of such a combined flat field.

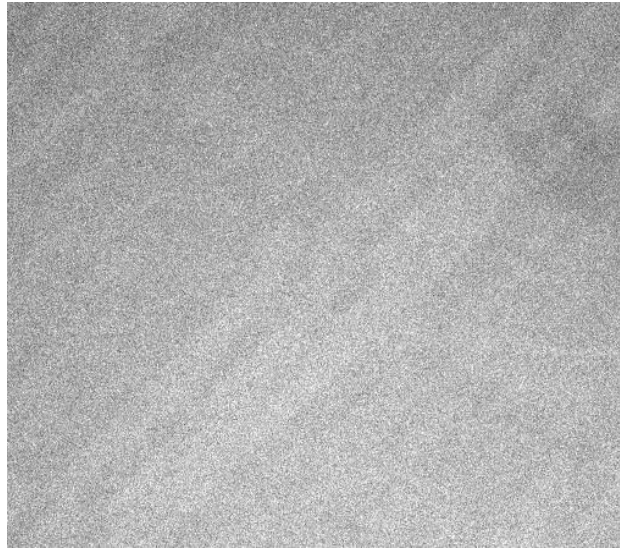


Figure 3.3 - CCD photometry image of a combined flat field

3.2 Centering and shifting frames

Due to the tracking unevenness of the telescope, the stars in all the frames are not located in the same pixels. Therefore the stars were relatively moved due to the tracking and pointing errors of the telescopes during the long sequence of repeated observations. Hence it is necessary to be aligned the frames to a common center for convenience in performing photometry. For each observations of B, V and R filters, the reference frame should be determined independently. Two bright stars are identified including the CC And as shown in the Figure (3.4). The coordinates of selected two stars are determined using the task `*imexamine` in IRAF workplace. The coordinates of these centering stars were fed into `*imcentroid` algorithm to calculate the pixel shifts of x and y (Δx and Δy) direction with respect to two centering stars for all the frames. This is shown in the Figure (3.5).

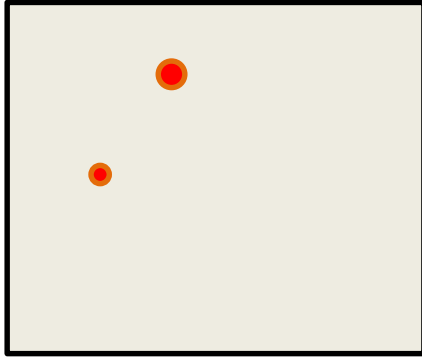


Figure 3.4 - Reference frame

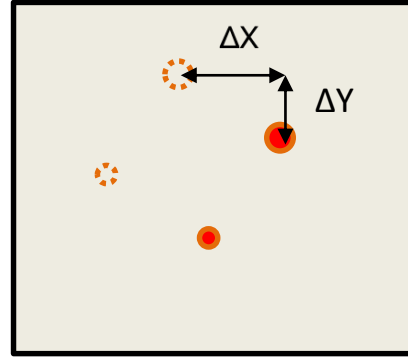


Figure 3.5 - Frame 1 (amount of shift with respect to reference frame)

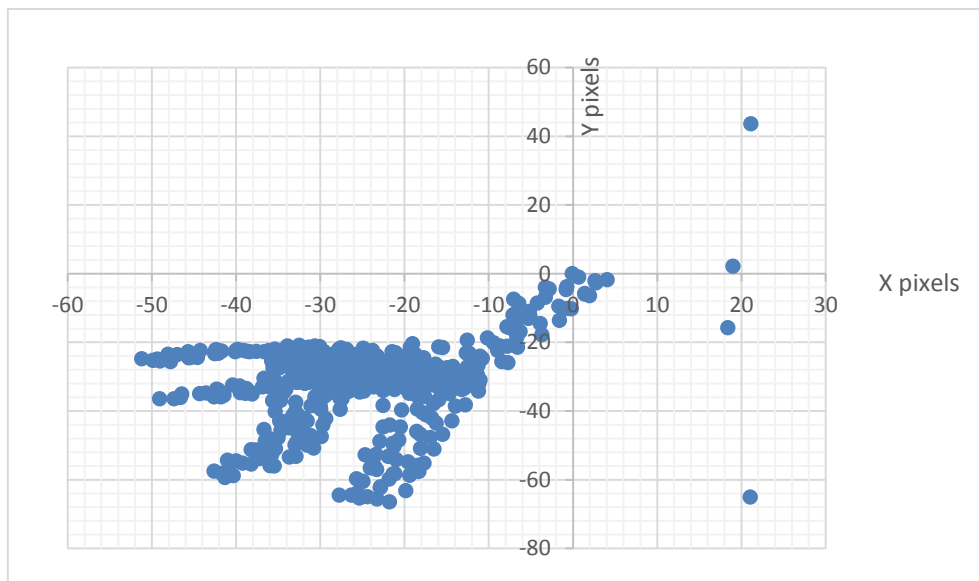


Figure 3.6 - Amount of shift of 538 frames of CC And with respect to the reference frame of (B band)

The next step is shifting. Figure (3.6) shows the amount of shift of 538 frames of CC And for B band with respect to the reference frame. This x and y shift of each frames are given to the *imshift algorithm in IRAF to align all the frames in to a common center. Sometimes the shift can be too high related to the given reference coordinates. For such type of cases, coarse centering cannot be performed by increasing coarse centering radius. Therefore a new reference frame should be introduced and centering is done based on new reference frame with the same procedure. Finally, all the centered subsets were again aligned to the foremost reference frame to make the entire frame set to a common center. The final result can be confirmed by displaying all frames using a script and marking region of the star using Ds9 window.

3.3 Aperture photometry

Aperture photometry and point spread function fitting (PSF) are the common techniques used for measuring instrumental magnitudes. Measuring instrumental magnitude by placing synthetic aperture around the star is known as aperture photometry. Images in a crowded star field such as the central regions of a globular cluster can be measured by using PSF technique. Instrumental magnitude of isolated CC And star was obtained using aperture photometry technique. The basic principle behind the aperture photometry is enclosing the star in a circular aperture of some radius, adding up all the light in that circle and subtracting the amount of light contributed by the sky background in that same circle area. Finally the brightness (magnitude) can be obtained.

3.3.1 Detecting bright stars

CC And is the brightest star when compared to other stars in the field. Before extracting the instrumental magnitudes, bright stars in the field are detected using the tasks *datapars and *daofind in *daophot package with some parameter editing such as Full Width at Half Maximum (FWHM) value, sigma for the sky, detection threshold value, minimum good data value and maximum good data value. FWHM value and sigma value for the sky are obtained using *imexamine. The radial profile gives the FWHM of the Gaussian profile of the selected star. In order to define a common FWHM value, the radial profiles of several bright stars were taken and then average FWHM is estimated. The radial profile gives the FWHM of the Gaussian profile of the selected star. Figure (3.7) shows a typical radial profile of CC And star. Similarly, several sigma values for the sky background is obtained and the average sigma value is estimated. Other values for the following parameters are given manually according to the correct requirements.

Detection threshold in sigma : When the task *daofind is examining the image it will use an annulus with a diameter equal to the FWHM to find the highest number of counts inside and then estimates the average background count behind the star. It subtracts the background count from the highest, and then divides that value by sigma. The higher the threshold, the fewer false stars will be identified. However, *daofind may not pick up other real stars if the threshold is too high.

Minimum and maximum good data value : minimum value should be very low and maximum should be very high.

Finally, *daofind gives coordinate files for each images, it contain x and y center values, some statistics and photometric data of detected stars.

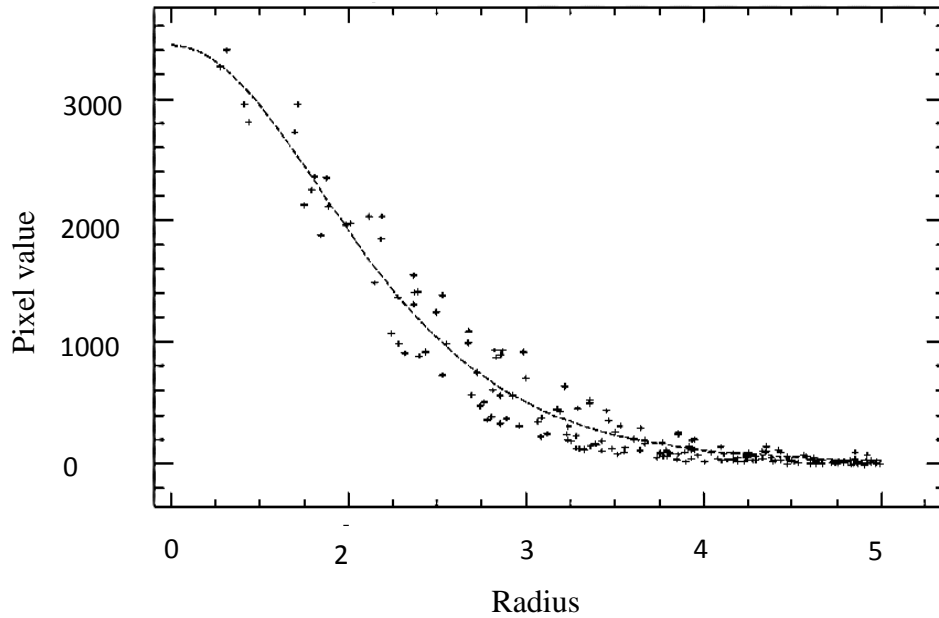


Figure 3.7 - A typical radial profile of CC And

3.3.2 Picking an aperture size

Picking an aperture size is significant in measuring the instrumental magnitudes of the star and aperture size should be big enough to include all of the light from the star. If the aperture size is too small, the light from the star cannot be counted and if it is too big, too much background or other stars can be counted. Automatically detecting the aperture is not available with IRAF. It should be done by examining the radial profiles of few images of the target star. The most basic rule to set an aperture radius is, 3 or 4 times the FWHM.

In IRAF, the algorithm *phot* is used to measure the magnitudes with several parameter editing to define the appropriate aperture. Aperture radius was obtained according to the above mentioned way. In addition to the aperture radius several parameters are defined. In order to model the value of the sky, the size and the location of the sky annulus have to be defined.

Inner radius of the sky was set 3 pixels away from the aperture and width of the sky was set to 5 pixels. The selected parameter values for *phot* are in Table (3.1). The following Figure (3.8) shows the arrangement of aperture parameters.

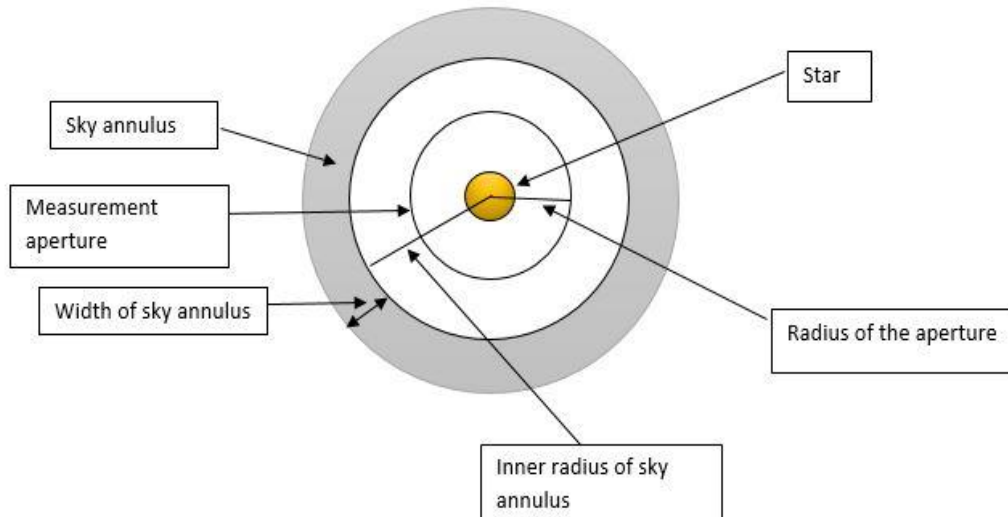


Figure 3.8 - The arrangement of aperture parameters

Table 3.1 Important parameters for extraction of instrumental magnitudes

	FWHM value	Aperture radii	Inner radius	Sigma
12 th November 2016				
B	4.49	13.5	16.5	11.48
V	4.58	13.74	16.74	15.21
R	4.73	14.19	17.19	12.72
13 th November 2016				
B	6.50	19.5	22.5	76.1
V	5.82	17.46	20.46	57.93
R	6.35	19.05	22.05	134.7

A separate text files for all image sets containing instrumental magnitudes were obtained for the data sets using the above parameters. Finally, the task **txdump* was used to extract the

magnitude from the text file (including CC And) and Julian Date (JD) was extracted from the header file.

3.4 Light curve analysis

3.4.1 Lomb-Scargle Periodogram light curve analysis

Instrumental magnitudes of CC And was directed to investigate the possible oscillation periods using VARTOOL software package [13]. The VARTOOLS program is a command line utility that provides tools for processing and analyzing astronomical time series data. Methods of calculating variability and periodicity statistics of light curves are available in VARTOOL. Lomb-Scargle (L-S) search of the light curves was performed for periodic sinusoidal signals. Lomb-Scargle periodogram [14] is a well-recognized algorithm for detecting and characterizing unevenly sampled data. The Lomb-Scargle period finding algorithm was applied on the light curves searched for periods between 0.01 and 1 days at a frequency resolution of $0.001/T$. T is the time-span of the light curve which is 0.171667 days for B, 0.17208 days for V and 0.17125 for R. The output was set to report the highest peak and periodogram was obtained. Each light curve was pre-written and re-applied L-S before finding the next peak and 5 sigma iterative clipping was used in determining the spectroscopic signal-to-noise. For each peak it will output the period found, the algorithm of the formal false alarm probability (LS probability) and the spectroscopic signal to noise ratio (SNR) for the peaks. ($SNR = (LS - \langle LS \rangle) / RMS(LS)$; where LS is the normalized statistics). LS probability is the log value of the false alarm probability that the probability of detecting a signal from noise. An unlike good fit which has a very small LS probability interpreted of detection of corresponding period. In order to process for the LS periodogram, the input text file should contained three columns namely Julian date, magnitude and the error of magnitude [15].

3.4.2 Light curves of BVR bands of CC And

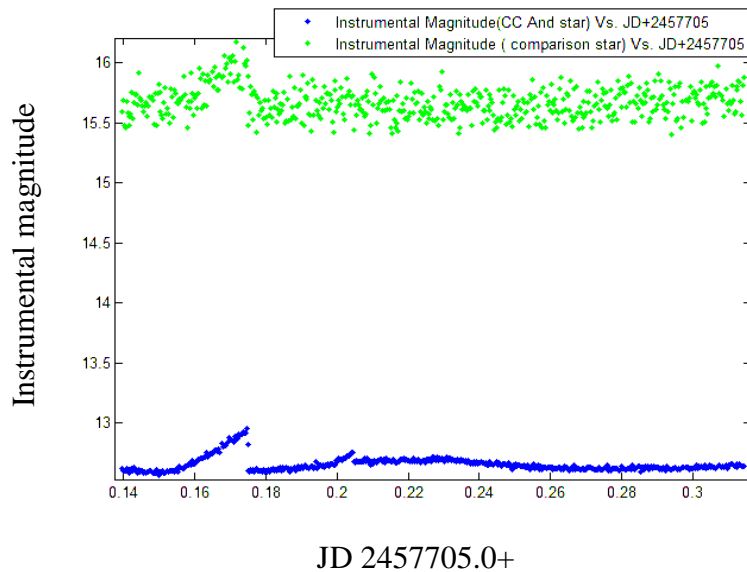


Figure 3.9 - Light curves of CC And variable star and comparison star in same plot (for B band)

Light curves for B, V, and R bands of CC And star and comparison star was obtained by plotting Instrumental magnitude vs. JD values using MATLAB. The light curves of comparison star and CC And for B band together is given on Figure (3.9) and separately given at Figure (3.10) and (3.11).

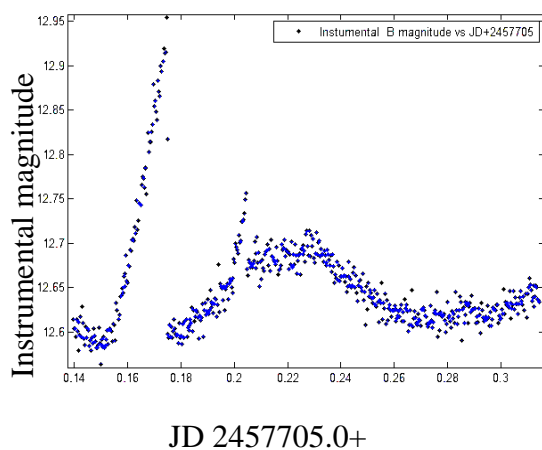


Figure 3.10 - Light curve of CC And of B band

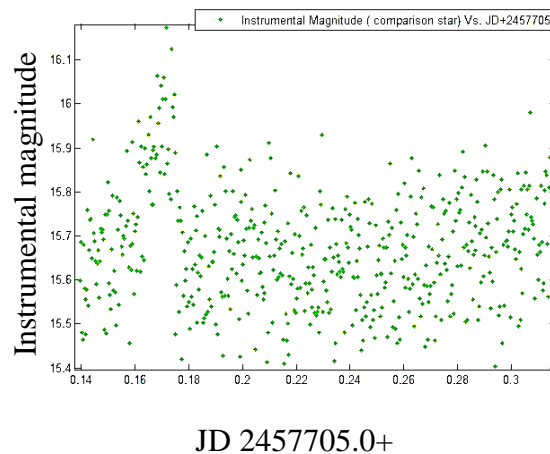


Figure 3.11 - Light curve of comparison star of B band

The sudden variations of light curves can be seen in all three bands (Fig. 3.12). This may occur due to some instrumental effect of measurements. Differential photometry can be performed to

reduce such type of error. But in this case comparison star does not show smooth variation in magnitude and its scatter is normally high. Therefore applying differential photometry would not improve the light curves of CC And. The instrumental and atmospheric magnitude anomalies were manually rejected and corrected light curves were used for further analysis.

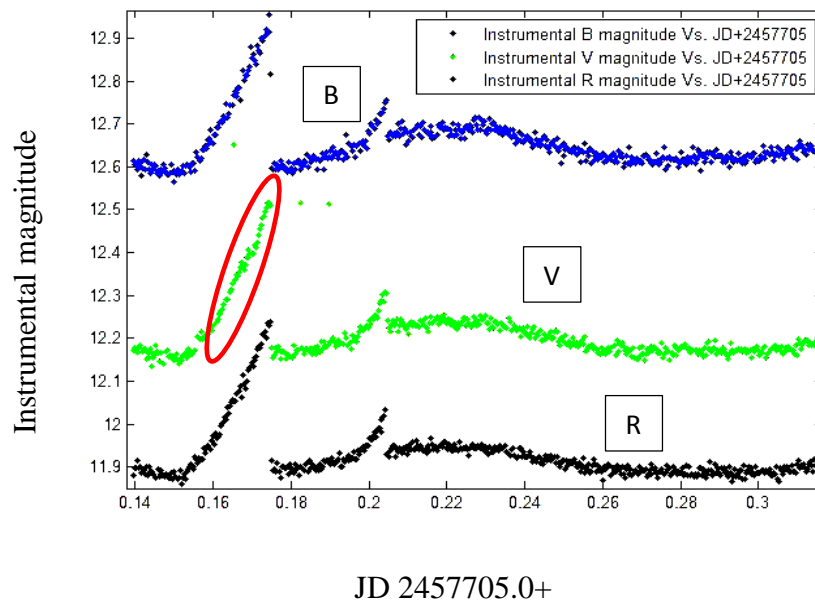


Figure 3.12 - Light curves of CC And for B, V, R bands

3.4.3 Fourier Analysis

Stars that shows periodic signal can be expressed as a Fourier series [16] of the form,

$$f(x) = a_0 + \sum_{n=1}^{\infty} (a_n \cos(n\omega t) + b_n \sin(n\omega t))$$

$f(x)$ – Observed magnitude at time t ,

a_0 – Mean magnitude

a_n, b_n – Amplitude components of $(n-1)^{\text{th}}$ harmonic

n – Order of the fit $n=1, 2, 3, \dots$

ω – Angular frequency

Oscillation period T can be calculated using,

$$T = 2\pi / \omega$$

Obtained light curves for B, V and R bands of variable star CC And were further subjected to Fourier analysis using MATLAB in order to get the general model for Fourier fitting. Fundamental component and other harmonic components can be determined through this model. The Figure (3.13) shows the Fourier fitting of CC And.

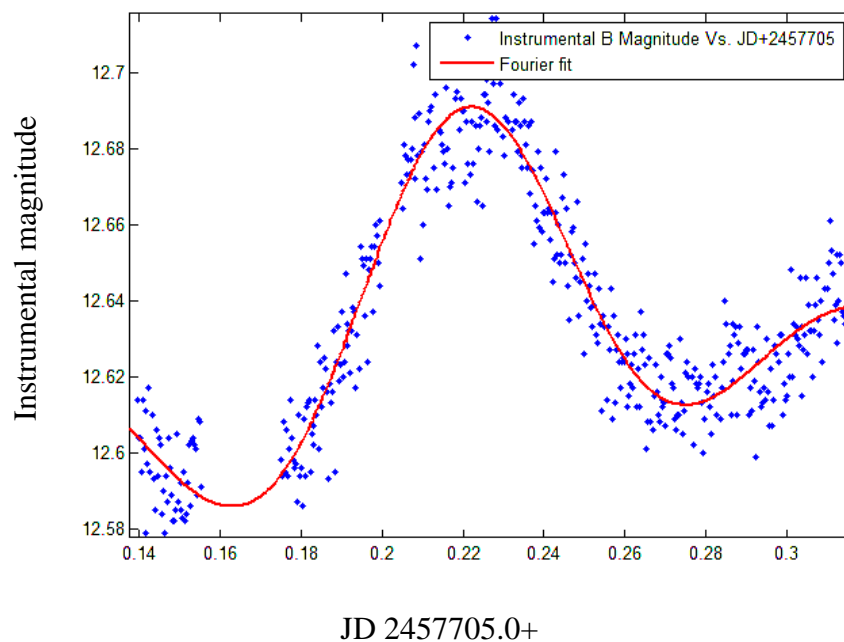


Figure 3.13 - Fourier fitting of B band light curve of CC And for 12th November 2016. The line shows the Fourier function fitted to the observed values (order = 3)

3.4.4 Detection of oscillation periods of BVR bands of CC And

The observations of CC And star was subjected for oscillation periods investigation. Fourier fitting with MATLAB gives a general model, coefficient values, angular frequency and goodness of fit values for the light curve. The fundamental frequency component and other harmonic frequency components were plotted and frequencies were calculated by using those values. Figure (3.14) shows the frequency components in B band of CC And for the 12th November data set.

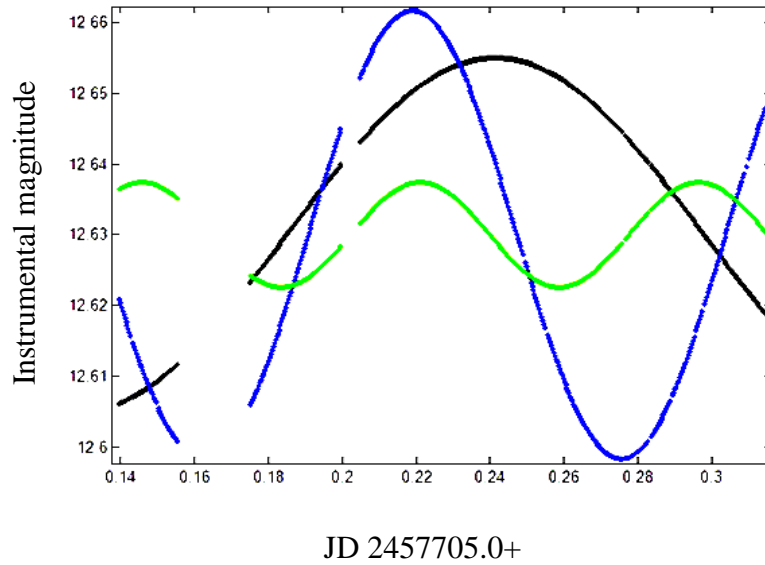


Figure 3.14 - Frequency components in B band of CC And for the 12th November data set

Blue and green color curves represents the fundamental and 1st harmonic respectively. The extensive observation of CC And have been subjected for oscillation period investigation using VARTOOLS. The data were investigated for primary and secondary frequencies. LS algorithm was run in order to search the periods between 0.01 and 1 with the frequency resolution of $0.01/T$ where T is the span of light curves. The process search for 6 peaks and used a 5 sigma iterative clipping in determining the spectroscopic signal to noise. The power spectrum of B was produced in the output. Accordingly, obtained results were given in Chapter 4.

CHAPTER 4

Results

4.1 Light curves of CC And

After extraction of instrumental magnitudes and Julian days of CC And, the data was fed into MATLAB to interpret the results. Periodic variations can be clearly identified in light curves of CC And of 12th November data set for B, V and R bands as shown in Figure (4.1), Figure (4.2) and Figure (4.3) respectively. The Figure (4.4) shows the light curves of CC And in same plot for B, V and R bands of 12th November photometric data. Also, the light curves of B, V and R bands of CC And of 13th November data set do not show periodic variations as shown in Figure (4.5), Figure (4.6) and Figure (4.7) respectively. The Figure (4.8) shows the light curves of CC And in same plot for B, V and R bands of 13th November photometric data.

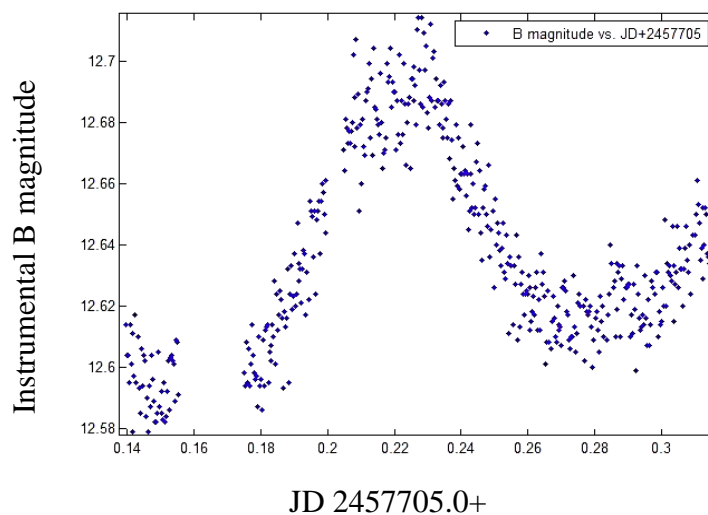


Figure 4.1 - Light curve of B band of CC And observed on 12th November 2016

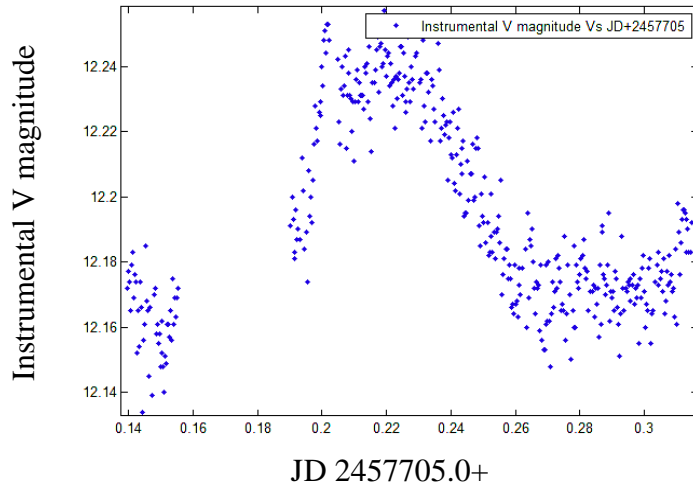


Figure 4.2 - Light curve of V band of CC And observed on 12th November 2016

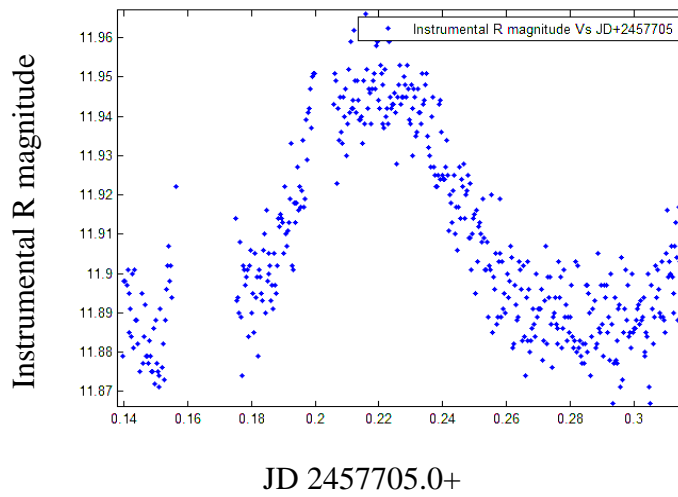


Figure 4.3 - Light curve of R band of CC And observed on 12th November 2016

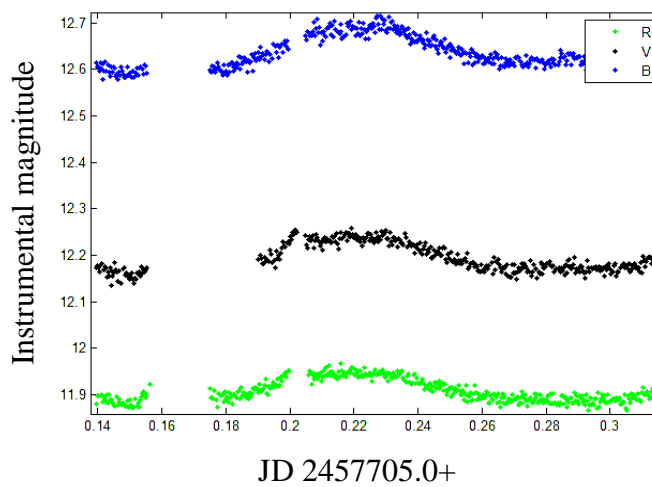


Figure 4.4 - Light curves in B, V and R bands of CC And observed on 12th November 2016 in same plot

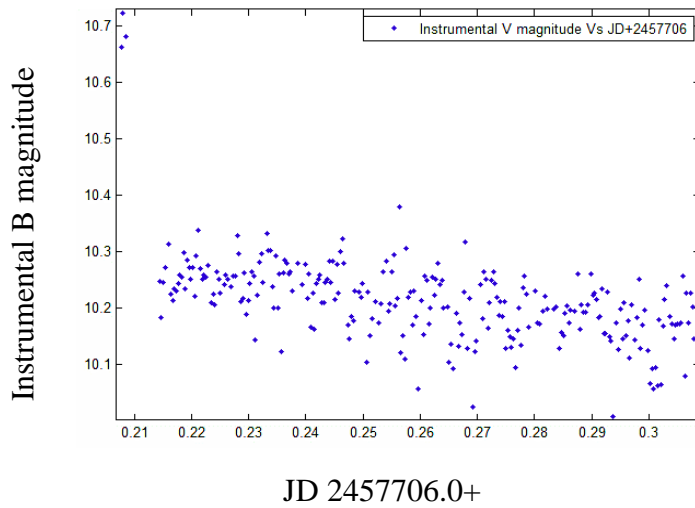


Figure 4.5 - Light curve of B band of CC And observed on 13th November 2016

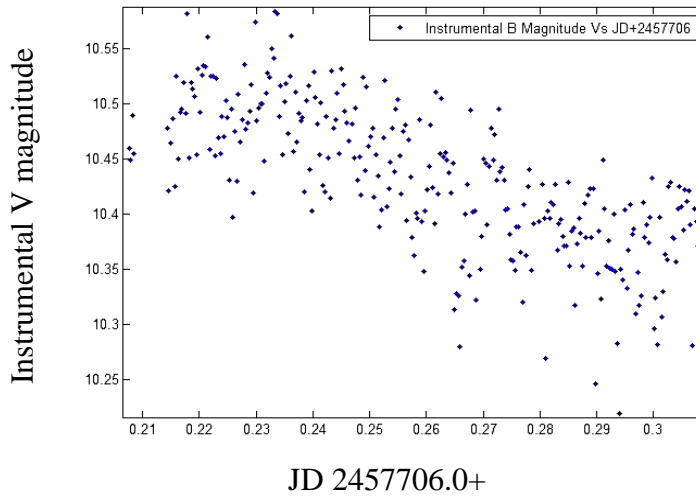


Figure 4.6 - Light curve of V band of CC And observed on 13th November 2016

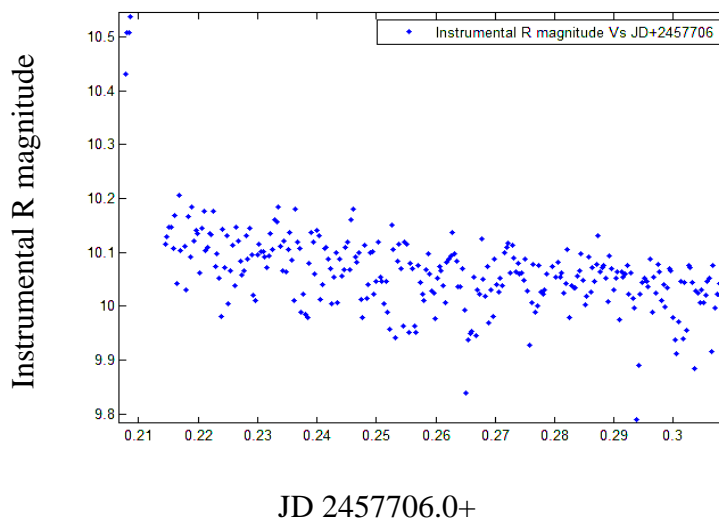


Figure 4.7 - Light curve of R band observed on 13th November 2016

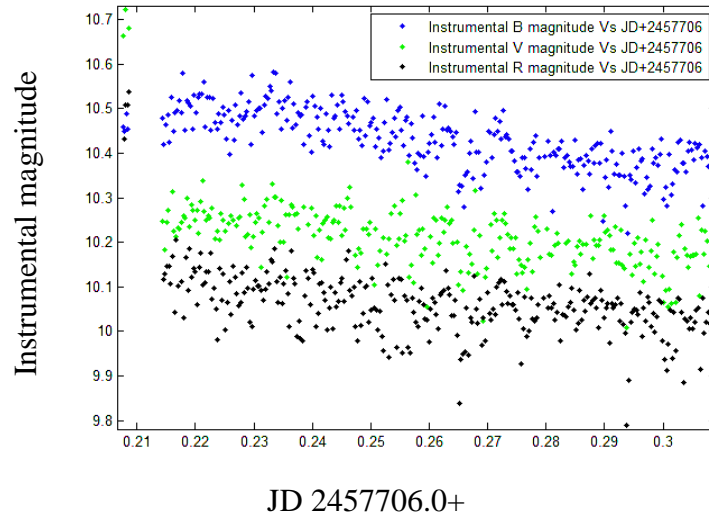


Figure 4.8 - Light curves in B, V and R bands of CC And observed on 13th November 2016 in same plot

4.2 Oscillation periods of CC And

The star CC And is Delta Scuti type variable star with main oscillation period of 0.1249078 days. Light curves in B, V, and R bands of Delta Scuti type variable star were examined separately to investigate main oscillation period and other oscillation periods using Fourier analysis. The graphical interpretation of Fourier fitting and frequency components in B, V and R light curves of CC And are shown in following Figure (4.9), Figure (4.10) and Figure (4.11) respectively.

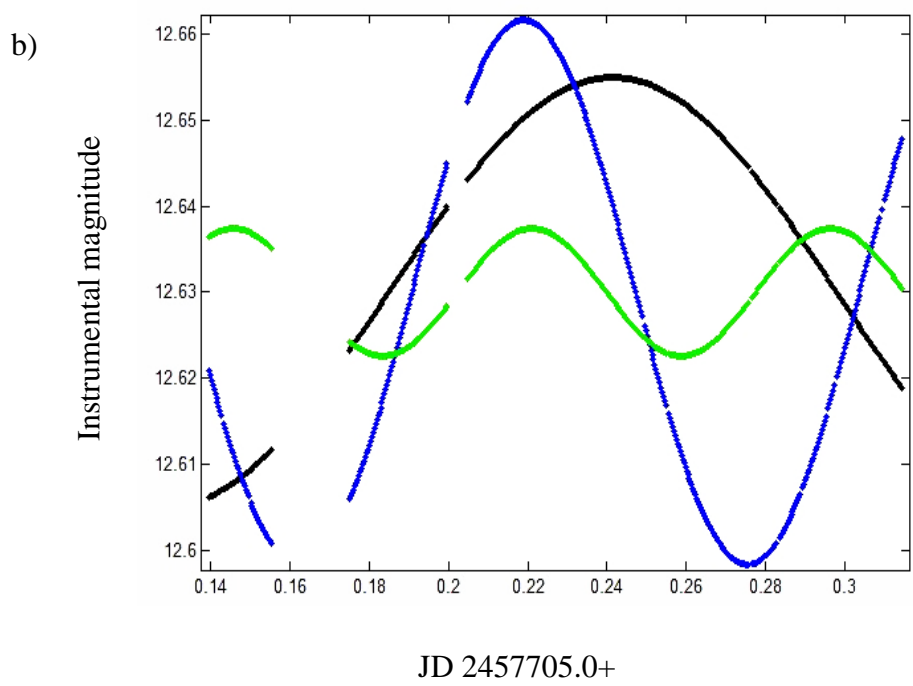
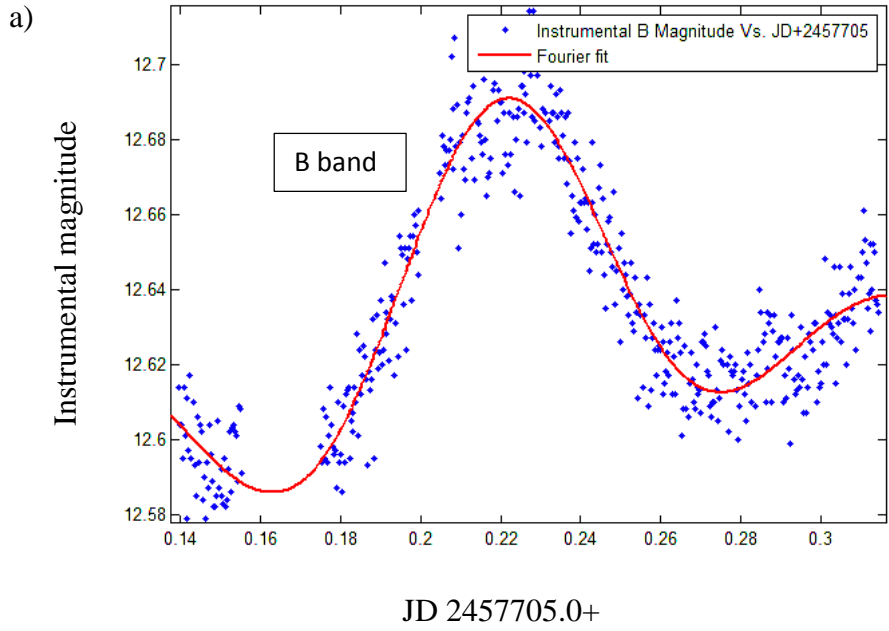


Figure 4.9 – (a) light curve, Fourier fitting, (b) corresponding frequency components in B band of CC And observed on 12th November 2016. Blue and green color curves represents the fundamental and 1st harmonic respectively.

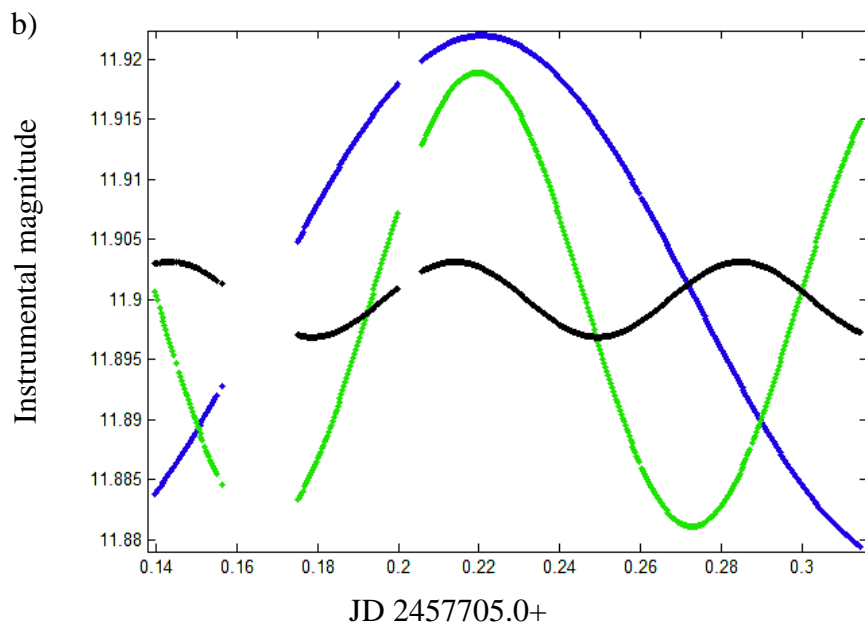
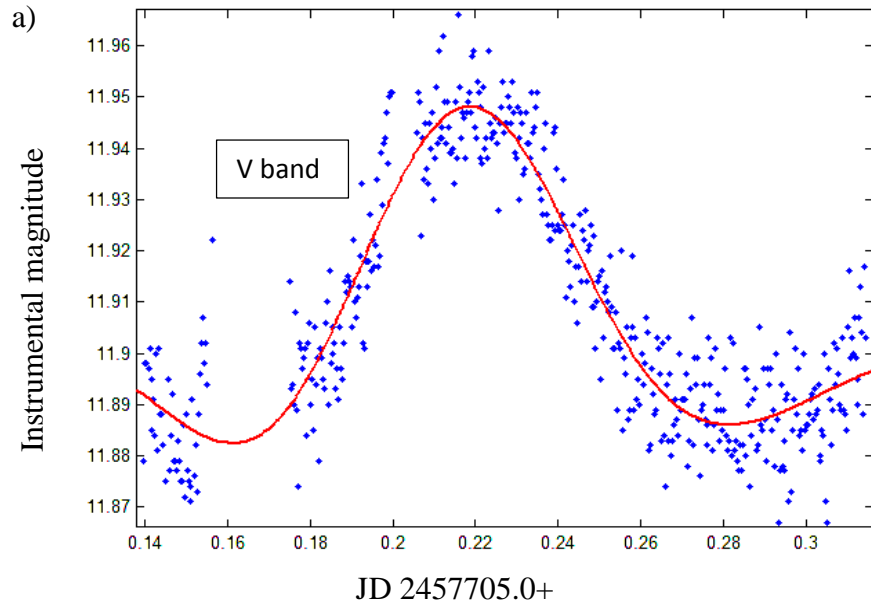


Figure 4.10 - (a) light curve, Fourier fitting, (b) corresponding frequency components in V band of CC And observed on 12th November 2016. Green and black color curves represents the fundamental and the 1st harmonic respectively.

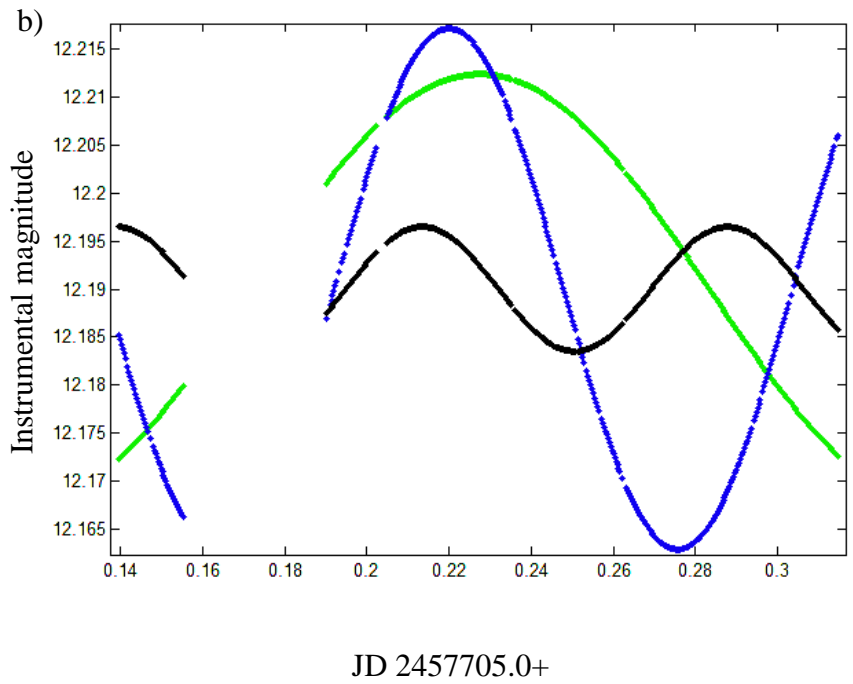
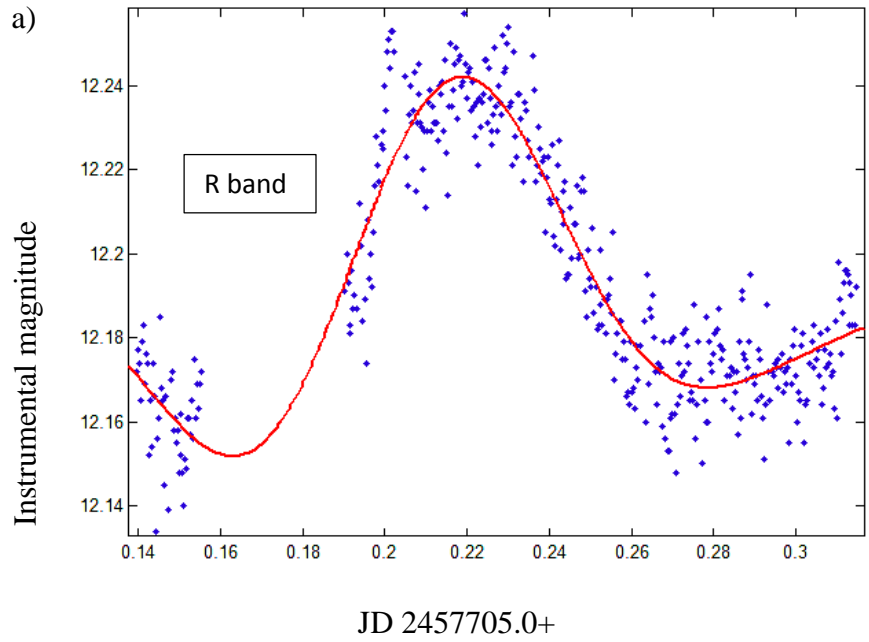


Figure 4.11 - light curve, Fourier fitting and corresponding frequency components in R band of CC And observed on 12th November 2016. Blue and black color curves represents the fundamental and the 1st harmonic respectively.

The calculated oscillation periods are shown in the following Table (4.1). P_0 and P_1 are the primary and secondary frequencies detected from Fourier analysis.

Table 4.1 Periodic time of CC And. Three oscillation periods were clearly identified and listed in the table below for each of the BVR bands.

12 th November 2016	B	V	R
P_0 (Days)	$(1.1 \pm 0.7) \times 10^{-1}$	$(1.1 \pm 0.3) \times 10^{-1}$	$(1.1 \pm 0.6) \times 10^{-1}$
P_1 (Days)	$(0.8 \pm 0.5) \times 10^{-1}$	$(0.7 \pm 0.3) \times 10^{-1}$	$(0.7 \pm 0.4) \times 10^{-1}$

The CC And is observed in B,V and R bands with high time resolution for detecting oscillations in addition to the main oscillation period. The observations of CC And were examined and pulsating periods were detected using Lomb-Scargle periodogram analysis. The LS power spectra of each oscillations of V, B and R bands of CC And are shown in the Figure (4.12), Figure (4.13) and Figure (4.14) respectively.

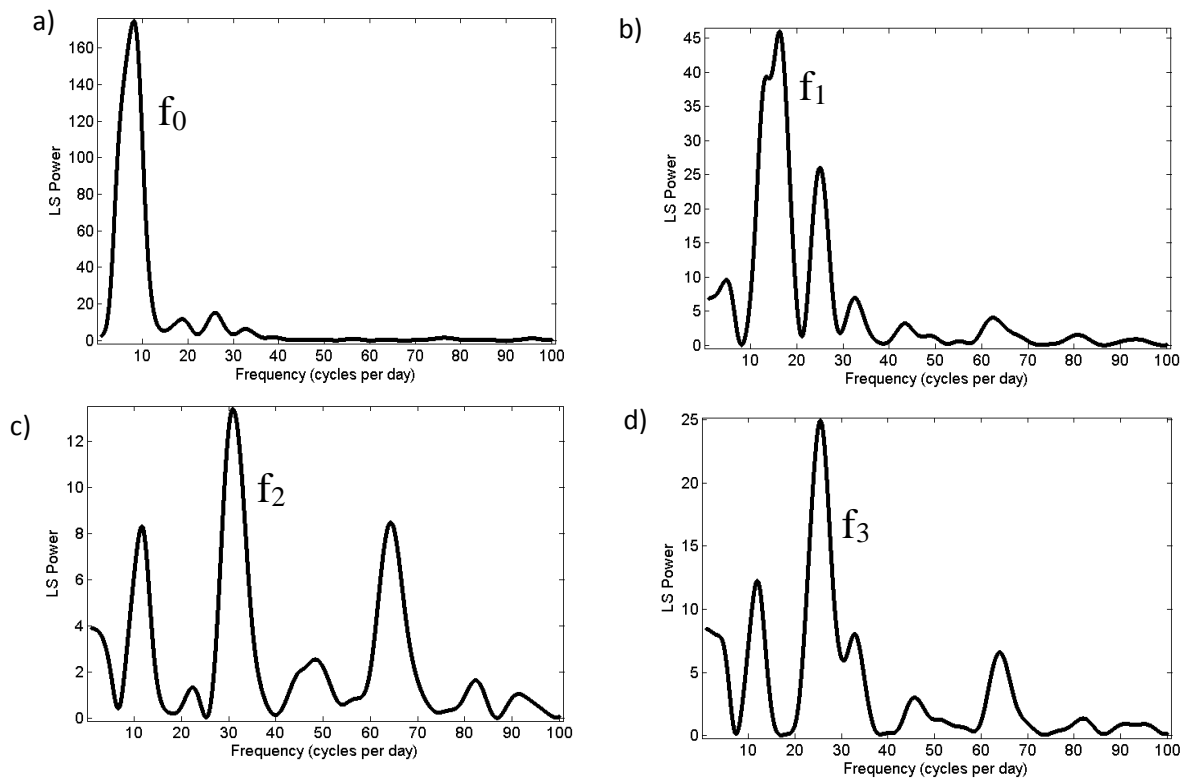


Figure 4.12 - L-S power spectra of V for the 12th November observations of CC And with frequencies f_0 , f_1 , f_2 and f_3

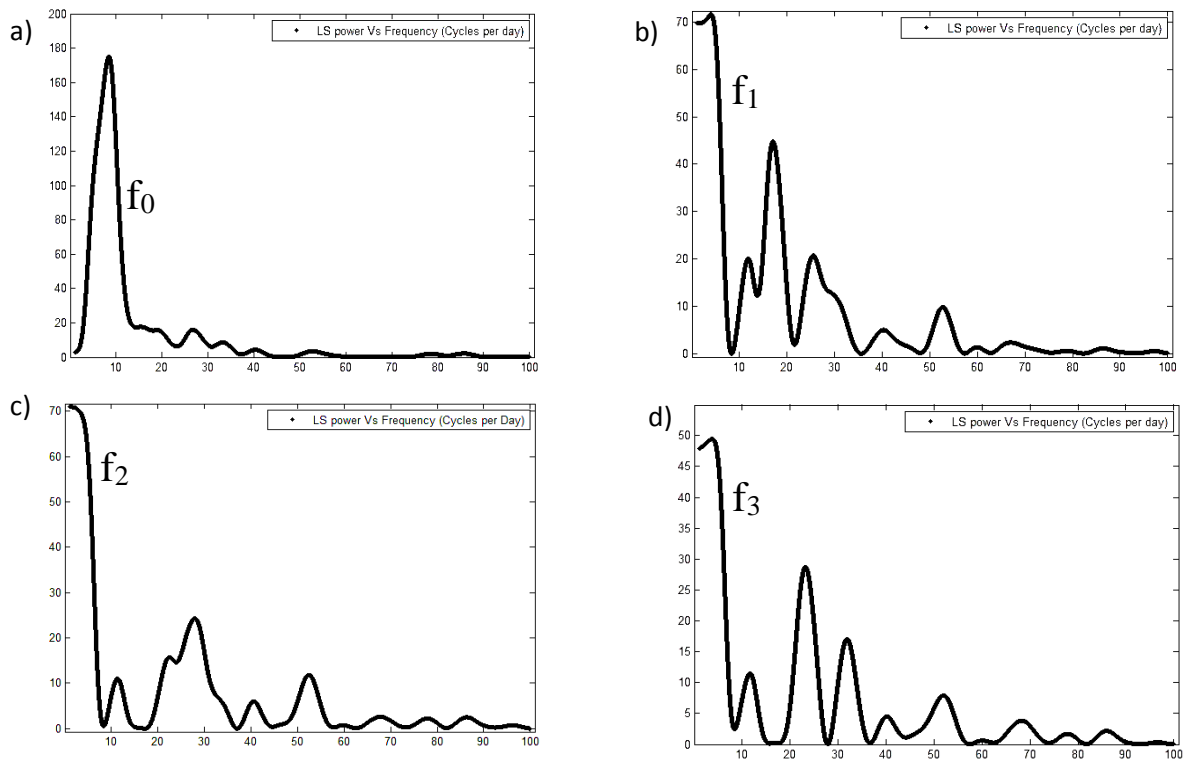


Figure 4.13 - L-S power spectra of B for the 12th November observations of CC And with frequencies f_0 , f_1 , f_2 and f_3

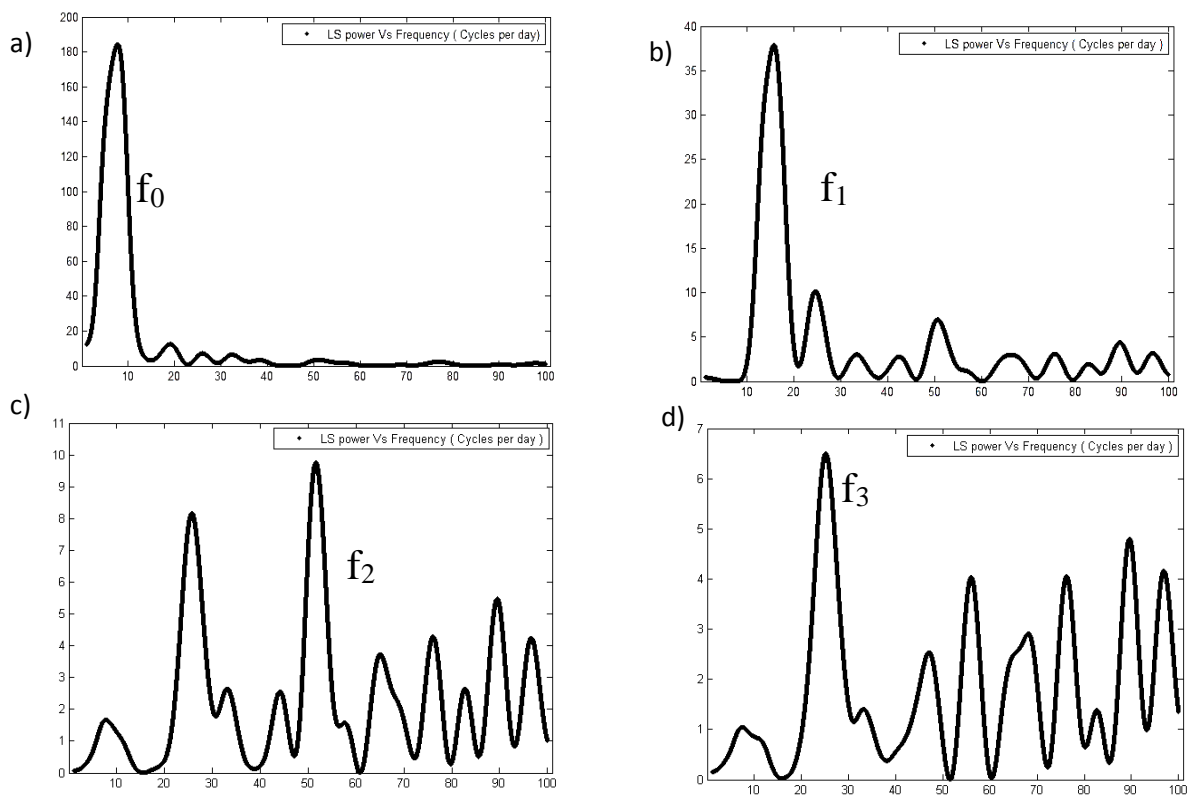


Figure 4.14 - L-S power spectra of R for the 12th November observations of CC And with frequencies f_0 , f_1 , f_2 and f_3

Five oscillation periods (P_0, P_1, P_2, P_3, P_4) of CC And for BVR filters were clearly identified and listed in the Table (4.2).

P_0 is the main oscillation period and P_1, P_2, P_3, P_4 , are the harmonics.

Table 4.2 The oscillation periods of CC And for BVR filters.

V	Period (Days)	LS Probability (log)	LS S/N Ratio
P_0	$(1.2 \pm 0.06) \times 10^{-1}$	-74.32	16.28
P_1	$(0.6 \pm 0.06) \times 10^{-1}$	-18.41	08.43
P_2	$(0.4 \pm 0.06) \times 10^{-1}$	-09.27	07.52
P_3	$(0.3 \pm 0.06) \times 10^{-1}$	-04.24	05.86
P_4	$(0.2 \pm 0.06) \times 10^{-1}$	-02.64	07.16
B	Period (Days)	LS Probability (log)	LS S/N Ratio
P_0	$(1.2 \pm 0.06) \times 10^{-1}$	-74.45	9.56
P_1	$(0.6 \pm 0.06) \times 10^{-1}$	-17.87	2.29
P_2	$(0.4 \pm 0.06) \times 10^{-1}$	-8.99	1.48
P_3	$(0.3 \pm 0.06) \times 10^{-1}$	-3.18	0.43
P_4	$(0.2 \pm 0.06) \times 10^{-1}$	-2.16	0.23
R	Period (Days)	LS Probability (log)	LS S/N Ratio
P_0	$(1.3 \pm 0.06) \times 10^{-1}$	-78.44	24.02
P_1	$(0.6 \pm 0.06) \times 10^{-1}$	-14.90	16.72
P_2	$(0.2 \pm 0.06) \times 10^{-1}$	-2.69	5.42
P_3	$(0.1 \pm 0.06) \times 10^{-1}$	-0.60	2.42
P_4	$(1.0 \pm 0.06) \times 10^{-1}$	-0.39	2.48

CHAPTER 5

Discussion and Conclusion

Oscillation periods were clearly identified in CC And for the 12th November photometric data. The light curves of B, V, and R bands were subjected to Fourier analysis and L-S periodogram algorithm to find out the possible oscillation periods. The main oscillation period for CCAnd obtained from Fourier analysis and L-S periodogram have shown in the summarized Table (5.1) below.

Table 5.1 Summary of main oscillation period of CC And for 12th November data.

METHOD	B	V	R
Fourier (Days)	0.1131698	0.1144351	0.1060274
Lomb- Scargle (Days)	0.1186401	0.1237511	0.1295610

Fourier analysis in B, V and R bands of CC And detected another oscillation period. Oscillation period of main frequency of V band, 0.1237511 that is obtained using Lomb-Scargle periodogram analyzing is approximated to the well-established period of 0.1249078 day. Also, in addition to the main pulsation period another four harmonic periods were detected by Lomb-Scargle period-finding algorithm. Lomb-Scargle period finding algorithm is the most commonly used method for calculating the spectrum of non-uniformly spaced data. It is more appropriate algorithm than the Fourier analysis for unevenly sampled data.

Also, a very low frequency was detected after using Fourier analyzing in B, V and R bands, oscillation period with 0.2263395, 0.2228870 and 0.2120549 respectively. In order to conform this low frequency we need at least two or three continuous cycles of data. The photometric observations of 12th November, there were only one cycle of the light curve of CC And. The analysis will be more accurate if there were two or more cycles within that light curve.

The following Figure (5.1) represents the light curve of CC And of B band for 13th November data which does not show clear periodic variation due to the high scattering of data points. The

V and R bands are also highly scattered which do not show clear variation. This data set probably taken in a photometrically non favorable condition. Therefore, further investigation of oscillation periods were not carried out for the 13th November data set.

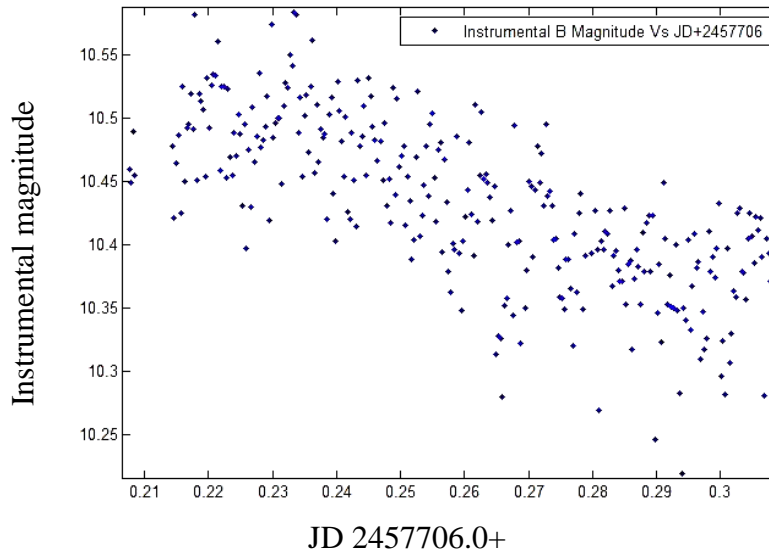


Figure 5.1- Light curve in band of CC And observed on 13th November 2016

The following Figure (5.2) shows the light curve of comparison star and the light curve of CC And for 12th November photometric data. Sudden variation among the light curve of comparison star and light curve of CC And can recognize (Fig 5.3). This error occurs due to instrumental effect or sudden variation of sky conditions and normally this can be reduced by performing differential photometry.

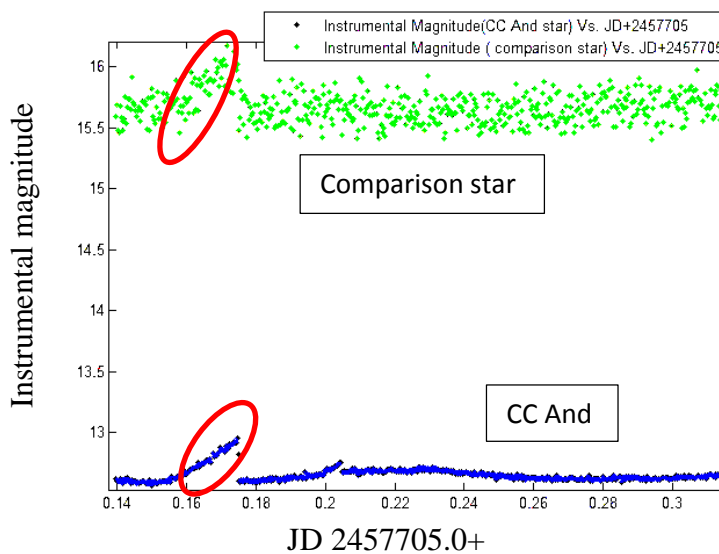


Figure 5.2 - Sudden variation in Comparison star and CC And star

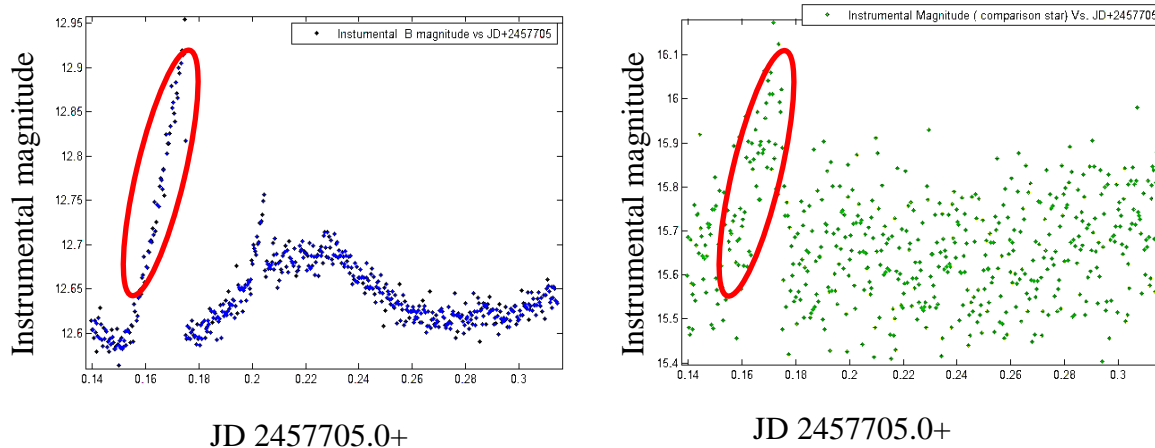


Figure 5.3 - Light curves of Comparison star and CC And with deviated data

Differential photometry is a straight forward method of performing photometry. It is simply the difference between the instrumental magnitude of the target star and the comparison star. Usually the comparison star must not show variation in magnitude. The result cancels out the instrumental effect in the measurements. This can be useful to investigate how the magnitudes of a star varies over time by plotting measurements in a light curve. Due to the non-smoothness and the high scattering of the comparison star, the resultant of differential photometry was not investigated for further analysis.

There are several limitations when observing a variable star. CC And is a most perfect one among those stars because the period of that star is not too large or small compared to others. CC And has an oscillation period approximately 3 hours. So the detection of one cycle of CC And within one night is comparatively easy among variable stars. The CC And shows 0.1 instrumental magnitude change which can be detected by simple CCD system. Therefore this target is possible to observe in medium scale telescopes.

The work we have done is successful, since we have obtained almost the same oscillation period for V band as previously calculated. The most important fact of the investigation is identifying the oscillation periods other than the fundamental period of CC And. For the best of our knowledge the study of secondary periods in B, V and R bands of CC And was not previously attempted and this study also shows the importance of carrying out Lomb-Scargle periodic analysis for the investigation of oscillation frequencies.

Appendix

Script files written in IRAF

```
/// This script is written to filter the images to B, V and R bands
separately and make list ///

while(fscan(list,s1)!=EOF){

imgets((s1),"FILTA")

s2= (imgets.value)

print((s1), >> (s2) // ".list")

print(s2)

}

/// This script is written to display all images in a list ///

list= "ListName"

while(fscan,(list,s1)!= EOF){

display(s1)

}

/// This script is used to extract JD from the header file and write
it to a text file ///

list="ListName"

while(fscan(list,s1)!=EOF){

imgets((s1),"JD")

s2=(imgets.value)

print((s2),>> "Bjdlist")    /*Bjdlist is a blank text file and it
                             has to be created before run the script*/

}
```

References

- [1] J. R. Percy, "Astrophysics and Space Science", variable stars in astronomical research, education and development, Vol. 258, Erindale College, University of Toronto, Mississauga, Ontario, Canada L5L 1C6, 1997, pp. 357–365.
- [2] Andriessen, M., Pentland, P., Gaut, R. & McKay, B. (2001). "Physics 2 HSC Course", Australia, Wiley, 2001, pp.326
- [3] Gondhalekar P. "The Grip of Gravity", Cambridge, Cambridge University Press, 2001, pp.530
- [4] A. Baglin, M. Breger, C. Chevalierx, B. Hauck, J.M. le Contel, J.P. Sareyanv and J.C. Valtier, "Delta Scuti stars", Observatoire de Nice, University of Texas at Austin, Observatoire de Meudon, Department d'Astrophysique Fondamentalex, Institut d'Astronomie de Universite de Lausanne et Observatoire de Geneve, Observatoire de ParisV, Departement de Photometrie. 1973, pp. 221-240.
- [5] O. C. Wilson and Merle F. Walker, "Simultaneous spectrographic and photometric observations of the short period variable SX Phoenix and CC Andromedae", Carnegie Institution of Washington, California Institute of technology, 1956, pp. 326-341
- [6] W. H. Fitch, "The light variation of CC Andromedae", Steward Observatory, University of Arizona, 1960, pp.701-715
- [7] S. Parimucha and M. Vanko, "Photometry of the variable stars using CCD detectors", Institute of Physics, Faculty of Natural Sciences, University of P.J. Saf'arik, 040 01 Ko sice, The Slovak Republic, Astronomical Institute of the Slovak Academy of Sciences 059 60 Tatransk'a Lomnica, The Slovak Republic, 2005, pp. 35-44.
- [8] E. Norman Walker, "CCD photometry", British Astronomical Association, para 2. [Online], Available: www.britastro.org/vss/ccd_photometry.html, [Accessed: July. 17, 2017].
- [9] M.S Bessell, "standard photometric system" Research School of Astronomy and Astrophysics, The Australian National University, Weston, 2005. pp. 293-336
- [10] M.S Bessell, "UBVRI passbands", Astronomical Society of the Pacific, vol. 102, Oct. 1990, pp. 1181-1199.
- [11] Janaka Adassuriya, "photometric study of short period variable star", Center for space science and Technology Education in Asia and Pasific (CSSTEAP), India, 2015, pp. 9.
- [12] Thijs Coenen and Yan Grange, "Running IRAF v.0.9", pp. 19

- [13] J. Hartman, The VARTOOLS Light Curve Analysis Program,
<http://www.astro.pinceton.edu>
- [14] N. R. Lomb, "Astrophysics and Space Science", School of Physics, University of Sydney, N. S. W., Australia, 1976, pp. 447-462.
- [15] Janaka Adassuriya, "photometric study of short period variable star", Center for space science and Technology Education in Asia and Pacific (CSSTEAP), India, 2015, pp. 24.
- [16] S. Deb and H. P. Singh, "Light curve analysis of variable stars using Fourier decomposition and principal component analysis", Department of Physics & Astrophysics, University of Delhi, Delhi 110007, India., 2009, pp. 1730-1739